Hindawi
Shock and Vibration
Volume 2021, Article ID 8996831, 10 pages
https://doi.org/10.1155/2021/8996831

Research Article

Estimating the Basal Heave Stability of Narrow Braced Excavations

Taoli Xiao,[1,2] **Yanlu Yang**,[3] **Hua Cai**,[4] **Shaoxin Yan**,[5] **and Fang Cao**[5]

[1]*State Key Laboratory of Geomechanics and Geotechnical Engineering, Institute of Rock and Soil Mechanics, Chinese Academy of Sciences, Wuhan 430071, China*
[2]*School of Urban Construction, Yangtze University, Jingzhou, Hubei 434023, China*
[3]*Sinopec Yantai LNG Co., Ltd, Yantai, Shandong 264000, China*
[4]*Bureau of Housing and Urban-Rural Development in Jingzhou, Jingzhou, Hubei 434023, China*
[5]*Jianghan Construction Projects Working Drawings Review Office in Jingzhou, Jingzhou, Hubei 434007, China*

Correspondence should be addressed to Taoli Xiao; 200536@yangtzeu.edu.cn

Received 10 May 2021; Revised 25 October 2021; Accepted 1 November 2021; Published 25 November 2021

Academic Editor: Erkan Oterkus

Engineering practices indicate that narrow braced excavation exhibits a clear size effect. However, the slip circle method in the design codes fails to consider the effect of excavation width on basal heave stability, causing waste for narrow excavation. In this paper, numerical simulation for basal heave failure of excavation with different widths was performed by FEM with SSRT (shear strength reduction technique). The results revealed that the failure mechanism of narrow excavation is different from the complete slip circle mode. In addition, the safety factor decreases increasingly slowly as the excavation widens and stabilizes when approaching the critical width. Subsequently, the corresponding computation model was presented, and an improved SCM (slip circle method) was further developed. Finally, the engineering case illustrated that it can effectively optimize the design, which exhibits clear superiority.

1. Introduction

In recent years, the construction of urban underground space in China has rapidly developed, and the proportion of narrow excavations, such as underground integrated pipe galleries, has been increasing sharply. This type of excavation shows an obvious size effect, with smaller deformation and better stability [1–7]. Tan and Wei [4] attributed this phenomenon to the narrow geometry, while the numerical simulation results indicated that narrower excavation has better support system stiffness [6]. Moreover, studies [5, 7] have suggested that with increasing excavation width, the deformations caused by excavation and pre-excavation dewatering first increase and subsequently tend to be stable. Logically, for narrow excavations, the support system can decrease accordingly [5]. Hosseinzadeh and Joosse [3] proposed a new design optimization method by quantifying the effect of overlapping passive zones.

Estimating the basal heave stability of braced excavation is quite significant for design. Up to the present, it can be performed by using the limit equilibrium method (LEM) [2, 8–19], limit analysis method [9, 20–24], probabilistic method [2, 10, 25–32], and finite element method (FEM) with shear strength reduction technique (SSRT) [2, 10, 15, 20, 33–40].

The limit equilibrium method can be divided into two categories [15, 19, 21, 24]: the bearing capacity method [8, 9, 13, 16, 17] and the slip circle method (SCM) [11, 16, 18, 19]. The stability models proposed by Terzaghi [17] and Bjerrum and Eide [8] are based on bearing capacity theory [2, 15, 19, 32, 40]. For these two types of methods, factors of safety (F_s) are both defined as the ratio of the resistance over the load [15, 34]. In principle, "failure" (the occurrence of excessive basal heave) is said to occur if $F_s < 1$. In practice, a minimum F_s is often required and is generally specified in design codes [12, 14, 16, 18].

Compared to the limit equilibrium method, the limit analysis method employs a plastic theory basis and can give strict upper and lower bounds for the ultimate load. Thus, its result is much more accurate than the former in many cases [9]. According to upper bound theory, Chang [9] revised Terzaghi's

method. Ukritchon et al. [22] summarized the formulation of numerical limit analyses that compute rigorous upper and lower bounds on the exact stability number. The results of the limit analyses provided an independent check on the accuracy of long-established empirical equations for computing the stability number of braced excavations.

The above two methods belong to deterministic approaches, where the soil parameters are generally taken as constant. Actually, because of the inherent variability of soil parameters (such as undrained shear strength and unit weight), which may lead to a slight difference between the actual circumstances and the theoretical assumptions, failure may still occur [28–29], even though the factors of safety (F_s) is greater than 1 or the minimum value specified in the design codes, such as undrained shear strength and unit weight [29]. To this end, probabilistic approaches have been developed based on the limit equilibrium method and limit analysis method. Reliability theory logically considers the uncertainty in the soil parameters [15], where the design variables are considered random in nature [25]. Many studies on reliability analysis [26, 28–32] have been carried out using the slip circle model [19] on account of its simplicity and suitability for modeling random fields [28]. Above all, it does not assume homogeneity [32]. Goh et al. [27] introduced basic structural reliability concepts to reflect the degree of uncertainty of the underlying random variables. Luo et al. [29] presented a simplified approach to consider the effect of spatial variability in a two-dimensional random field. Wu et al. [31] adopted a nonstationary random field to model the spatial variability of undrained shear strength.

Naturally, with the continuous development of computer and numerical methods, FEM with SSRT has been widely applied to geotechnical engineering and has gradually become the mainstream numerical method and effective means for the analysis of complex engineering problems. In this way, many scholars [2, 10, 20, 33, 35–39] evaluated the basal heave factors of safety for excavations and analyzed the influence of various factors.

The current design codes [13, 16] consider that excavations with different widths have the same basal heave factors of safety, resulting in huge design waste. Therefore, FEM with SSRT was used to simulate the basal heave failure of excavations with different widths in this paper. The factors of safety and the failure surfaces were obtained. Furthermore, an improved approach based on the slip circle mode was presented. Eventually, it was verified by engineering case analysis.

2. Basal Heave Analysis for Narrow Excavations

SCM has been widely adopted by building codes in Japan [12], mainland China [13, 14, 16], and Taiwan [18] for a long period and has proven to be reliable based on past experiences [11]. As shown in Figure 1, it assumes a circular failure arc with a prescribed trajectory extending from a point at the base of the excavation in front of the pile to a point at the lowest strut level (point O) behind the pile [26]. In this method, F_s can be expressed by taking moments about the lowest strut level [2, 10, 11, 28]:

$$F_s = \frac{M_r}{M_d}, \tag{1}$$

where M_r is the resisting moment and M_d is the driving moment. As revealed in Figure 1, H is the excavation depth, D is the penetration depth, R is the radius of the failure circle, q is the surcharge, and W is the total weight of the soil mass behind the pile and above the excavation level. The failure circle is fixed with a center at the lowest strut and passes through the end of the pile.

For a general wide excavation, the failure surface of the slip circle in Figure 1 largely conforms to the actual situation. However, when the excavation is narrow enough (width B less than $[D(D+2d)]^{1/2}$), the development of the slip circle will be restrained by the support piles on the other side. In terms of symmetry, the damaged soil wedge in the passive zone changes from sector MSQ to trapezoidal with a curved side MNPQ, and the support piles on both sides interact with each other. The horizontal reaction on side PN makes the soil wedge tight and difficult to slip; accordingly, the passive earth pressure increases, and the basal heave stability is improved to some extent. When the excavation is wider, the constraint effect produced by the support piles on the other side becomes increasingly weaker until $B = [D(D+2d)]^{1/2}$, at which point it completely disappears. In this way, if the algorithms in current design codes continue to be employed, only taking the retaining structure on one side with the soil in active and passive zones as the research objects would certainly cause waste. Consequently, it is essential to consider the effect of excavation width.

3. Numerical Simulation

3.1. Basic Principle. The FEM with SSRT was proposed by Zienkiewicz et al. [41] for the initial purpose of calculating the stability of slopes. Later, it was successfully introduced into studies of the basal heave stability of excavation.

In essence, when the pressure difference between the inside and outside of the excavation exceeds the ultimate bearing capacity, the excavation will be unstable. Therefore, the damage can be attributed to excessive load or insufficient shear strength. The FEM with SSRT exactly simulates the failure process by reducing the strength parameters (cohesion c and tangent value of the internal friction angle φ) of the soil. The basic principle is that after c and $\tan\varphi$ are divided by the same reduction coefficient F_r [34], they are resubstituted into the numerical model as a new set of strength parameters for calculation to determine whether the excavation has reached the ultimate failure state, and the process is repeated until the excavation is in the limit equilibrium. At this time, the reduction coefficient F_r is the basal heave factor of safety F_s [2, 20, 33, 36].

$$\begin{aligned} c_r &= \frac{c}{F_r}, \\ \varphi_r &= \tan^{-1}\left(\frac{\tan\varphi}{F_r}\right), \end{aligned} \tag{2}$$

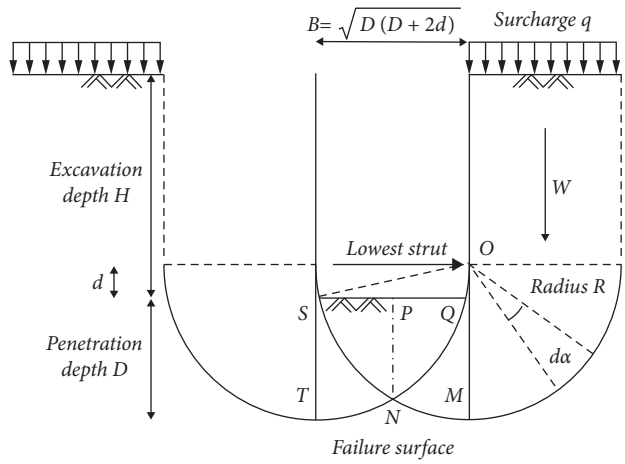

Figure 1: SCM for basal heave analysis.

where c and $\tan\varphi$ are the original shear strength parameters of soils, c_r and φ_r are reduced shear strength parameters, and F_r is the reduction coefficient.

Specifically, the key point of employing the FEM with SSRT to evaluate basal heave stability is to judge when the excavation reaches the ultimate failure state. The nodal displacement method as an evaluation criterion has been widely employed [20, 26, 33, 34, 36–38] for a long time, and it has good engineering applicability [34]. Its principle is as follows: through numerical calculation, the variation characteristics of the relationship between nodal displacement and the reduction coefficient are obtained. When the reduction coefficient increases to a certain value, the nodal displacement increases sharply, and it is considered that the excavation is unstable at this time. The physical meaning of the criterion is clear, and the solution is definite. Consequently, it was adopted in the present study.

In comparison to conventional methods, the most significant advantage of FEM with SSRT is that the failure surface and factor of safety emerge naturally without the user hypothesizing a particular failure mechanism in advance [15, 20, 33–36]. To explore the basal heave failure mechanism of narrow excavation, this section will perform numerical simulation through the FEM with SSRT.

3.2. Simulation Process. The simulation was carried out using the finite element software ABAQUS. Although it does not have a built-in SSRT program, it is still easy to implement. The essence of FEM with SSRT is to reduce the strength of materials continuously, while in ABAQUS, the parameters of materials can vary with field variables. Specific steps are as follows.

Step 1. Define a field variable, which is usually taken as the strength reduction coefficient F_r.

Step 2. Define material parameters that varied with the field variable.

Step 3. Specify the initial value of the field variable and apply a gravity load to the model to establish a stress balance state.

Step 4. In the subsequent analysis step, the field variable F_r gradually increases; after the calculation terminates (the numerical calculation does not converge), the results are processed, and the factor of safety is determined.

To consider the effect of B, the whole braced excavation was taken for analysis during the simulation, instead of only half due to symmetry [2, 10, 15, 33, 34, 37, 39]. In this study, plane strain analyses [10, 15, 37, 38, 40] were adopted to explore the configuration of failure surfaces and evaluate the basal heave factors of safety with different excavation widths. H and D of all cases analyzed are 8 m and 6 m, respectively, and B is the only variable. All excavations were retained by bored piles with a diameter of 800 mm and two inner struts. The first is a rectangular concrete strut with a length of 600 mm and width of 400 mm, and the second is a steel pipe with an outer diameter of 609 mm and a thickness of 12 mm, which were placed 0.4 m and 2.9 m below the ground, respectively. Total stress analysis was performed by using the Mohr–Coulomb model [2, 10, 20, 33, 36, 39]. The strut and pile elements were assumed to be linearly elastic. The grid was divided in an uneven way. That is, the elements near the excavation are denser, which can improve the calculation accuracy. The model consists of 1213 elements and 1218 nodes. The soil was modeled by 4-noded bilinear plane strain quadrangular elements, and the retaining structure (struts and piles) was modeled by 2-noded plane linear beam elements [42]. Tied constraints were adopted between the soil and retaining structure. The nodes along the side boundaries of the mesh were constrained from displacing horizontally, while the nodes along the bottom boundary were constrained from moving horizontally and vertically [2, 10, 15, 39]. Reduced Gaussian integration was used to avoid numerical difficulties, known widely as "locking" [20, 33, 36, 38]. The reduction coefficient varied from 0.5 to 7, and the material parameters are shown in Table 1. In the analyses, the stage-by-stage excavation of the soil and the installation of the struts were simulated [37, 38].

Table 1: Physical and mechanical parameters of materials.

Materials	Properties					
	H (m)	Γ (kN/m^3)	μ	E (kPa)	C (kPa)	Φ (°)
Steel	/	78	0.3	$2.00E+08$	/	/
Concrete	/	25	0.2	$3.00E+07$	/	/
Miscellaneous fill	2.8	18	0.4	7.00E+03	10	12
Silty clay	11.2	19	0.3	$1.30E+04$	18	16

3.3. Results and Discussion. The basal heave factor of safety F_s is generally used to evaluate the stability of a braced excavation. As previously mentioned, F_s determined by FEM with SSRT is the ratio of the original shear strength to the reduced shear strength when large nodal deformation occurs.

Figure 2 shows the variation of nodal displacement with the increase of shear strength reduction coefficient when $B = 6$ m. Due to the large safety reserve, at the beginning of strength reduction, the nodal displacement is always very small, almost zero. However, as the strength reduction process continues, the shear strength begins to be insufficient to maintain the stability of the excavation. When F_r is greater than 3.68, the nodal displacement increases sharply, and basal heave failure occurs. Naturally, the basal heave factor of safety is 3.68.

Figure 3 reveals the relationship between the basal heave factor of safety and excavation width. There are obvious nonlinear characteristics: the narrower the excavation is, the greater the factor of safety will be, and as the excavation widens, F_s decreases increasingly slowly. When $B = 10$ m (very close to the theoretical critical width of 9.86 m), F_s tends to be stable, and the effect of B is small enough to be ignored. This result demonstrates that the theoretical analysis above is comparatively reasonable, and neglecting the influence of excavation width would certainly cause considerable design waste.

This study is focused on identifying the configuration of a failure surface for the subsequent development of the new limit equilibrium method for a narrow braced excavation. For the FEM with SSRT, the failure surface is the connective zone of plastic shear strain. The failure surfaces obtained by numerical simulations for various cases are shown in Figure 4. There is good symmetry, and the failure surfaces approximately extend to the lowest strut level. For narrow excavations, the shape is half of a circle whose size increases linearly with excavation width ($R = B/2$) plus a vertical line segment. Moreover, the centers of the arcs are always located at the end of the support piles. Compared to the former, the shape of failure surface of wide excavation is a nonstandard semiarc, the intersection of the failure surfaces on both sides in the middle of the excavation moves up obviously, the interaction correspondingly weakens, and the centers of the arcs are no longer located at the end of the support piles. The simplified computation model developed from the simulation results is displayed in Figure 5. To describe the difference in passive earth pressure with various widths, the function factor K_{pf} is presented, $K_{pf} = 2B^2/(D^2+2Dd)$.

4. Improved SCM considering the Excavation Width

4.1. Basic Assumptions. According to the basal heave failure mechanism of narrow excavation, the basic assumptions are as follows:

(1) Because of the large strength and stiffness of the braced structure [20, 33, 36–38], the failure surface passes under the support pile.

(2) The shear strength of soil is analyzed by Mohr–Coulomb theory and computed by $\tau = \sigma\tan\varphi + c$.

(3) Considering the stratification of the soil mass, the moments are calculated separately first and then superimposed.

(4) The normal stress on the failure surface comprises the component force of the soil weight and the component force of the horizontal lateral pressure. Given that it is difficult to determine the stress state of soil after deformation occurs and that the horizontal lateral pressure in the active zone is between the active earth pressure and the earth pressure at rest, its approximate value is taken as $\gamma z\tan^2(45^\circ - \varphi/2)$ instead of subtracting $2c\tan(45^\circ - \varphi/2)$. Similarly, the horizontal lateral pressure in the passive zone takes $\gamma z\tan^2(45^\circ + \varphi/2)$, and the value does not include $2c\tan(45^\circ + \varphi/2)$.

(5) In practice, the contribution of the bending moment of the pile to the safety factor is so small that it is often neglected [35].

4.2. Formula Derivation. On the basis of the method in the existing design code in Shanghai [16] and based on the computation model developed from the numerical simulation, the formula derivation is completed. As shown in Figure 6, the soil body, which lies below the lowest strut level and above the assumed surface (the *PNMGFEQ* area), is taken for equilibrium analysis. The failure surface consists of vertical segment *FG*, *NP*, and arc *GMN*. The driving moment M_d is caused by the weight of the soil and possible surcharge, in which the weights within the areas GOM and NOM are offset by each other. The resisting moment M_r arises from the shear strength along the failure surface. Thus, the factor of safety F_s can be defined as equation (1), and the details are as follows:

$$M_r = M_{\mathrm{FG}} + M_{\mathrm{GM}} + M_{\mathrm{MN}} + M_{\mathrm{NP}},$$
$$M_d = M_{\mathrm{AC}} + M_{\mathrm{ACFE}} + M_{\mathrm{EFGO}} - M_{\mathrm{NPQO}}, \quad (3)$$

where M_{ACFE}, M_{EFGO}, and M_{NPQO} are the moments caused by the weight of the soil within the corresponding area.

$$\begin{aligned}
M_{\mathrm{FG}} &= \sum \int_{H_I}^{H_K} \tau_{\mathrm{FG}} \mathrm{R} \mathrm{dh},\\
\tau_{\mathrm{FG}} &= (q + \gamma h) K_a \tan \varphi + c,\\
K_a &= \tan^2\left(45^\circ - \frac{\varphi}{2}\right),\\
M_{\mathrm{GM}} &= \sum \int_{\alpha_I}^{\alpha_K} \tau_{\mathrm{GM}} R^2 d\alpha,\\
\tau_{\mathrm{GM}} &= [q_1 + \gamma(R \sin \alpha + h_0 - H_I)]\sin^2 \alpha \tan \varphi\\
&\quad + [q_1 + \gamma(R \sin \alpha + h_0 - H_I)]\cos^2 \alpha K_a \tan \varphi + c,\\
\alpha_I &= \arctan\left[\frac{H_I - h_0}{\sqrt{R^2 - (H_I - h_0)^2}}\right],\\
\alpha_K &= \arctan\left[\frac{H_K - h_0}{\sqrt{R^2 - (H_K - h_0)^2}}\right],\\
h_0 &= H + D,\\
M_{\mathrm{MN}} &= \sum \int_{\alpha_I}^{\alpha_K} \tau_{\mathrm{MN}} R^2 d\alpha,\\
\tau_{\mathrm{MN}} &= [q_2 + \gamma(R \sin \alpha + h_0 - H_I)]\sin^2 \alpha \tan \varphi\\
&\quad + [q_2 + \gamma(R \sin \alpha + h_0 - H_I)]\cos^2 \alpha K_p \tan \varphi + c,\\
K_p &= \tan^2\left(45^\circ + \frac{\varphi}{2}\right),\\
M_{\mathrm{NP}} &= \sum \int_{H_I}^{H_K} \tau_{\mathrm{NP}} \mathrm{R} \mathrm{dh},\\
\tau_{\mathrm{NP}} &= \gamma \mathrm{h} K_p K_{\mathrm{pf}} \mu + c,\\
K_{\mathrm{pf}} &= 2 - \frac{B^2}{D(D + 2\,d)},\\
M_{\mathrm{AC}} &= \frac{1}{2} \mathrm{q} \mathrm{R}^2.
\end{aligned} \quad (4)$$

The formula in area *ACFE* is identical to EFGO and NPQO:

$$M = \sum \int_{H_I}^{H_K} \frac{1}{2} \gamma R^2 \mathrm{dh} = \sum \frac{1}{2} \gamma R^2 (H_K - H_I), \quad (5)$$

where γ, c, φ, and μ are the unit weight, cohesion, angle of internal friction, and friction coefficient, respectively; q = surcharge; q_1 and q_2 are the overlying pressures outside and inside the excavation, respectively; h_0 is the depth of the center of the slip circle; H_I and H_K are the depths of the

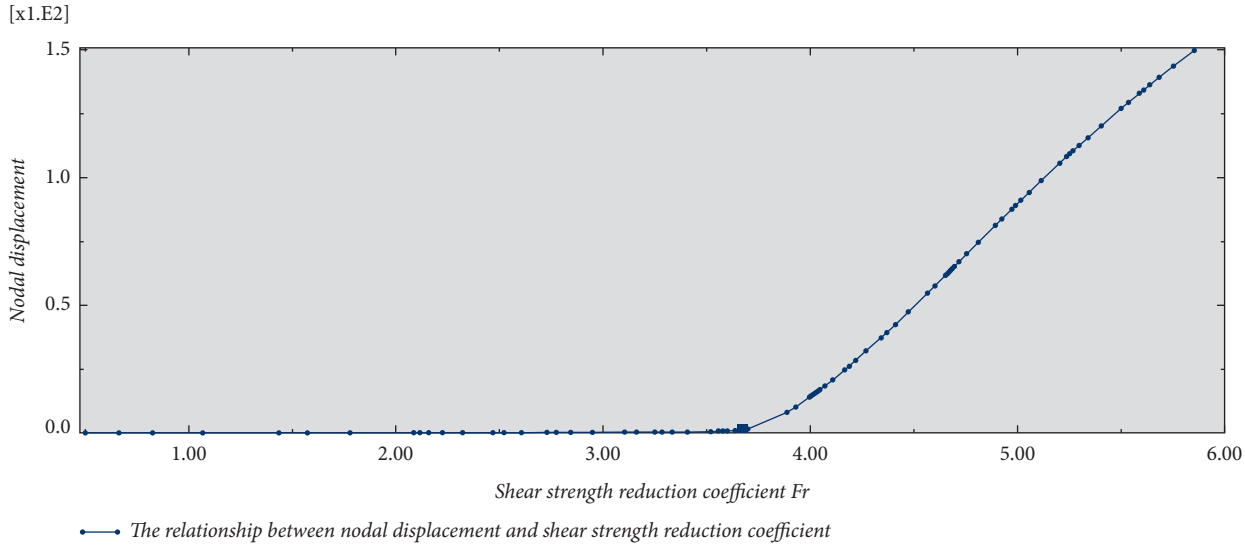

Figure 2: Basal heave factor of safety of excavation when $B = 6$ m.

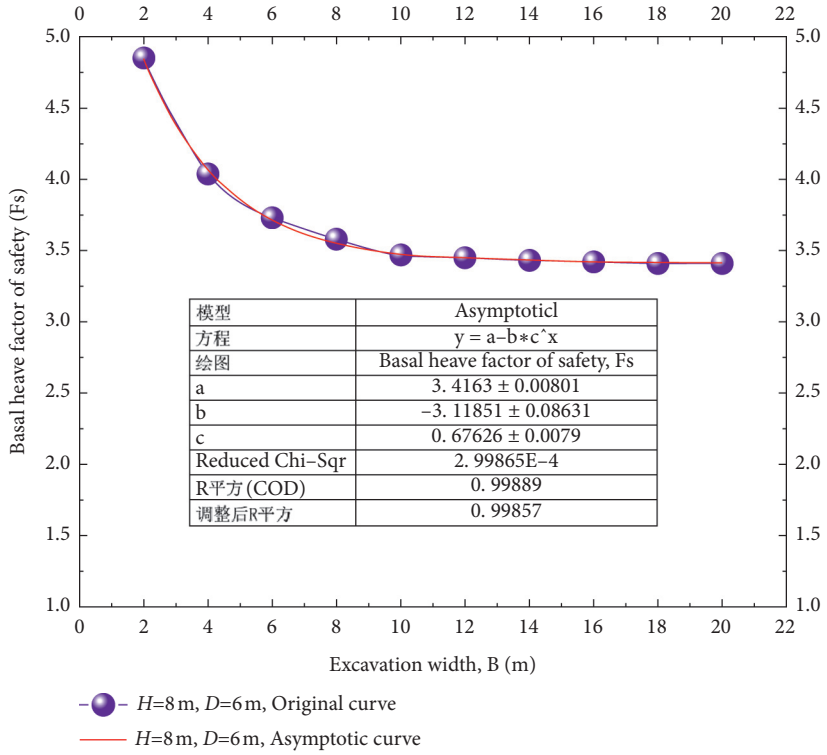

Figure 3: Influence of excavation width on basal heave stability.

upper and lower surfaces of the soil layer; α_I and α_K are the angles shown in the above figure; K_a and K_p are the active and passive earth pressure coefficients; and K_{pf} is the play factor of passive earth pressure for narrow excavation.

4.3. Verification. The cross section of the excavation of an underground integrated pipe gallery project in Jingzhou is revealed in Figure 7. $H = 12$ m, $B = 6$ m, $D = 8$ m, $d = 4$ m, and $q = 20$ kPa. Bored piles and inner struts were used to support. The pile was 800 mm in diameter and 1200 mm in spacing, and a crown beam of 1000 × 800 mm was set on the top of the pile. Three struts were adopted: the first concrete strut of 400 × 600 mm was poured with the crown beam, and the second and third were both steel pipes with outside diameters of 609 mm and thicknesses of 12 mm, which were at depths of −4 m and −8 m, respectively. The soils can be divided into four layers: (1) fill layer; (2) mucky silty clay layer; (3) silty clay layer; and (4) mucky silty clay layer. The properties of the soil layers are shown in Table 2.

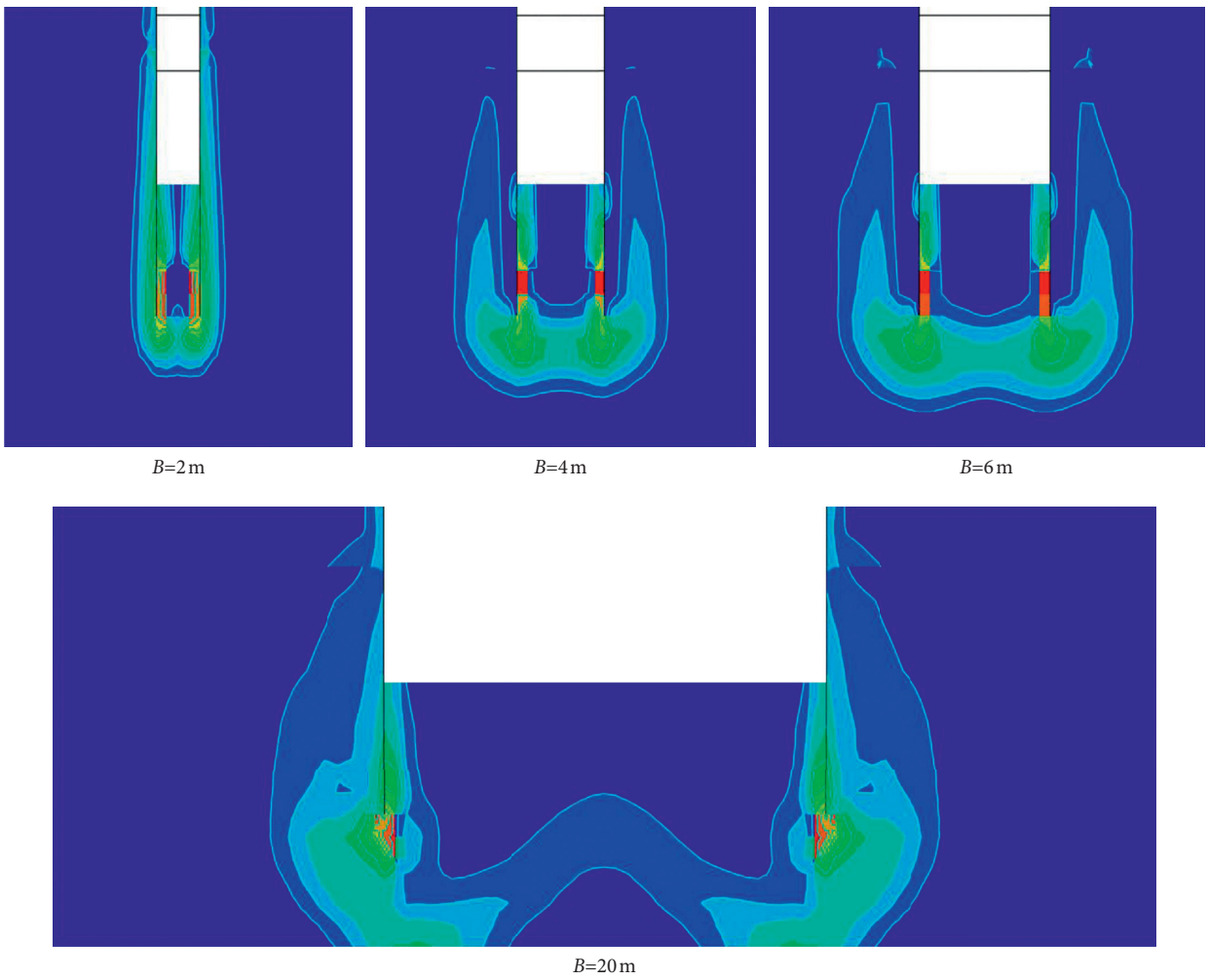

Figure 4: Configuration of failure surfaces. (a) $B = 2$ m. (b) $B = 4$ m. (c) $B = 6$ m. (d) $B = 20$ m.

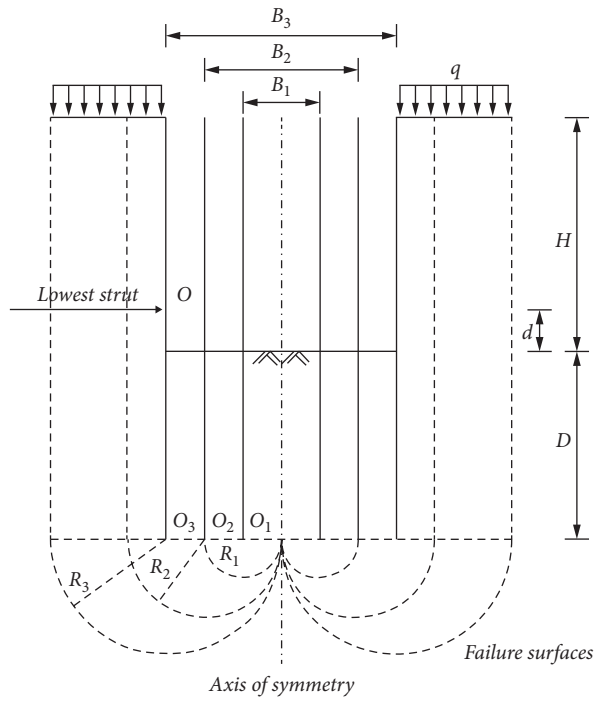

Figure 5: Simplified computation model for basal heave analysis of narrow excavations.

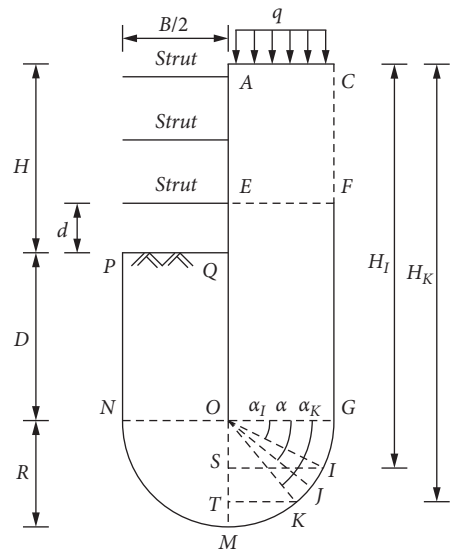

Figure 6: Schematic diagram to estimate the basal heave stability of narrow excavation.

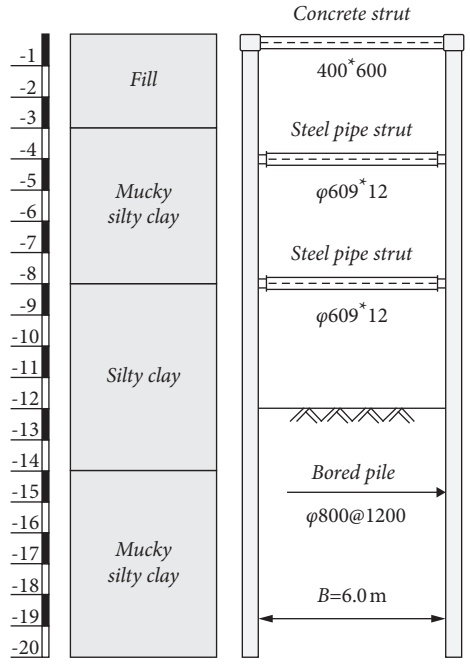

Figure 7: Cross section of the integrated pipe gallery excavation.

The proposed method was employed to estimate the basal heave stability of the narrow excavation above. The result is presented in Figure 8. The trends of the curves well reflect the size effect on the basal heave stability and are in accordance with engineering experiences, which means that narrower excavation tends to be more stable. When the penetration depth of the support pile is 8 m and the excavation width decreases from 8 m to 6 m, the basal heave factor of safety increases from 3.40 to 4.25, an increase of 25.0%. In contrast, to meet the requirement of a safety factor of 4.25, compared with the excavation with a width of 8 m, the penetration depth can be reduced from 10 m to 8 m when the width is 6 m, resulting in savings of 20.0%. This demonstrates that the proposed method can realize design optimization for narrow excavation, further leading to good economic and social benefits.

Table 2: Parameters of the soil mass.

Soil layers	H (m)	Γ (kN·m^{-3})	C (kPa)	Φ (°)	μ	K_a	K_p
Fill	3.0	17	7	7	/	/	/
Mucky silty clay	5.0	18	8	5	/	/	/
Silty clay	6.0	19	14	10	0.2	0.70	1.42
Mucky silty clay	6.0	18	10	4	0.1	0.87	1.15

Note. h = thickness; γ = unit weight; c = cohesion; φ = angle of internal friction; μ = friction coefficient; K_a = coefficient of active earth pressure; K_p = coefficient of passive earth pressure.

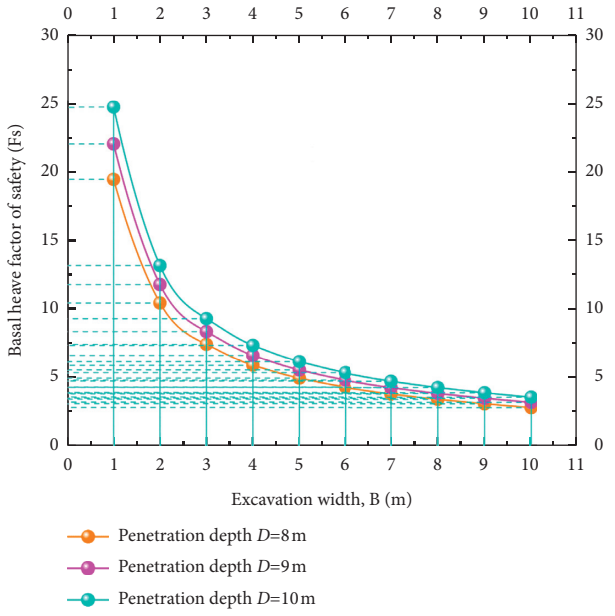

Figure 8: Basal heave analysis performed by the proposed method.

5. Conclusions

In this paper, an improved SCM (slip circle method) is proposed based on numerical simulation; it is applicable to evaluate the basal heave stability of narrow braced excavations. Subsequently, the approach has been tested by engineering cases, and the following conclusions are drawn on the basis of the presented results:

(1) To study the size effect of excavation, FEM with SSRT was adopted to simulate basal heave failure with different widths, and the safety factors were estimated according to the nodal displacement method. It was found that there exists a critical excavation width, and the safety factor increases nonlinearly with the decrease in width within the range of critical values.

(2) The configuration of the failure surface of narrow excavation exhibits half of a circle whose size increases linearly with excavation width plus a vertical line segment extending to the lowest strut level. Moreover, the center of the arc is always located at the end of the support pile.

(3) According to the simulation results, the computation model of basal heave stability was presented, and the improved SCM considering the effect of excavation width was further derived. This method can significantly improve the safety factor of narrow excavation and optimize the design, which shows obvious superiority.

Data Availability

The data used to support the findings of this study are included within the article.

Conflicts of Interest

The authors declare that there are no conflicts of interest regarding the publication of this paper.

Acknowledgments

This study was supported by the Open Research Fund of the State Key Laboratory of Geomechanics and Geotechnical Engineering, Institute of Rock and Soil Mechanics, Chinese Academy of Sciences (grant no. Z020013), Study on Failure Mechanism and Grouting Reinforcement Technology of Pipe Jacking Excavation in Overlying Water-Rich Sand Layer, Hubei Province (grant no. 2020AC15), and Science and Technology Planning Project of Jingzhou (grant no. 2019AC27).

References

[1] Z. Ding, J. Jin, and T.-C. Han, "Analysis of the zoning excavation monitoring data of a narrow and deep foundation pit in a soft soil area," *Journal of Geophysics and Engineering*, vol. 15, no. 4, pp. 1231–1241, 2018.

[2] A. T. C. Goh, "Deterministic and reliability assessment of basal heave stability for braced excavations with jet grout base slab," *Engineering Geology*, vol. 218, pp. 63–69, 2017.

[3] S. Hosseinzadeh and J. F. Joosse, "Design optimisation of retaining walls in narrow trenches using both analytical and numerical methods," *Computers and Geotechnics*, vol. 69, pp. 338–351, 2015.

[4] Y. Tan and B. Wei, "Observed b of a long and deep excavation constructed by cut-and-cover technique in Shanghai soft clay," *Journal of Geotechnical and Geoenvironmental Engineering*, vol. 138, no. 1, pp. 69–88, 2012.

[5] H. Xiao, S. Zhou, and Y. Sun, "Wall deflection and ground surface settlement due to excavation width and foundation pit classification," *KSCE Journal of Civil Engineering*, vol. 23, no. 4, pp. 1537–1547, 2019.

[6] X. H. Yang, M. C. Jia, and J. Z. Ye, "Method for estimating wall deflection of narrow excavations in clay," *Computers and Geotechnics*, vol. 117, Article ID 103224, 2020.

[7] C.-F. Zeng, G. Zheng, X.-F. Zhou, X.-L. Xue, and H.-Z. Zhou, "Behaviours of wall and soil during pre-excavation dewatering under different foundation pit widths," *Computers and Geotechnics*, vol. 115, Article ID 103169, 2019.

[8] L. Bjerrum and O. Eide, "Stability of strutted excavations in clay," *Géotechnique*, vol. 6, no. 1, pp. 32–47, 1956.

[9] M.-F. Chang, "Basal stability analysis of braced cuts in clay," *Journal of Geotechnical and Geoenvironmental Engineering*, vol. 126, no. 3, pp. 276–279, 2000.

[10] A. T. C. Goh, W. G. Zhang, and K. S. Wong, "Deterministic and reliability analysis of basal heave stability for excavation in spatial variable soils," *Computers and Geotechnics*, vol. 108, pp. 152–160, 2019.

[11] P.-G. Hsieh, C.-Y. Ou, and H.-T. Liu, "Basal heave analysis of excavations with consideration of anisotropic undrained strength of clay," *Canadian Geotechnical Journal*, vol. 45, no. 6, pp. 788–799, 2008.

[12] Jsa, *Guidelines of Design and Construction of Deep Excavation*, Japanese Society of Architecture, Tokyo (Japan), 1988.

[13] *Technical Specification for Retaining and protection of Building Foundation Excavations. JGJ120–2012*, Ministry of Housing and Urban-Rural Development of the People's Republic of China, Beijing (China), 2012.

[14] Pscg, *Specification for Excavation in Shanghai Metro Construction*, Professional Standards Compilation Group, Shanghai (China), 2000.

[15] Y. Sun, S. Zhou, and Z. Luo, "Basal-heave analysis of pit-in-pit braced excavations in soft clays," *Computers and Geotechnics*, vol. 81, pp. 294–306, 2017.

[16] "Technical code for excavation engineering. DG/TJ08–61–2018," Shanghai Management Commission of Urban-Rural Construction, Shanghai (China), 2018.

[17] K. Terzaghi, *Theoretical Soil Mechanics*, Wiley, New York, 1943.

[18] Tgs, *Design Specifications for the Foundation of Buildings*, Taiwan Geotechnical Society, Taipei (Taiwan), 2001.

[19] M. Zhang, Z. Zhang, Z. Li, and P. Li, "Axisymmetric arc sliding method of basal heave stability analysis for braced circular excavations," *Symmetry*, vol. 10, no. 5, p. 179, 2018.

[20] H. Faheem, F. Cai, K. Ugai, and T. Hagiwara, "Two-dimensional base stability of excavations in soft soils using FEM," *Computers and Geotechnics*, vol. 30, no. 2, pp. 141–163, 2003.

[21] Z. Tang, M.-s. Huang, and J.-y. Yuan, "Basal stability analysis of braced excavations with embedded walls in non-homogeneous clay by a kinematic approach," in *Proceedings of the GeoShanghai 2018 International Conference: Advances in Soil Dynamics and Foundation Engineering*, pp. 570–579, Springer, Singapore, 06 May 2018.

[22] B. Ukritchon, A. J. Whittle, and S. W. Sloan, "Undrained stability of braced excavations in clay," *Journal of Geotechnical and Geoenvironmental Engineering*, vol. 129, no. 8, pp. 738–755, 2003.

[23] L. Wang and F. Long, "Base stability analysis of braced deep excavation in undrained anisotropic clay with upper bound theory," *Science China Technological Sciences*, vol. 57, no. 9, pp. 1865–1876, 2014.

[24] J.-h. Zhang, T. Ling, Y.-q. Rao et al., "Limit analysis of basal heave stability in unsaturated soils based on the unified strength theory," *Geotechnical & Geological Engineering*, vol. 39, no. 1, pp. 593–602, 2020.

[25] S. S. Chowdhury, "Reliability analysis of excavation induced basal heave," *Geotechnical & Geological Engineering*, vol. 35, no. 6, pp. 2705–2714, 2017.

[26] J. Ching, K.-K. Phoon, and S.-P. Sung, "Worst case scale of fluctuation in basal heave analysis involving spatially variable clays," *Structural Safety*, vol. 68, pp. 28–42, 2017.

[27] A. T. C. Goh, F. H. Kulhawy, and K. S. Wong, "Reliability assessment of basal-heave stability for braced excavations in clay," *Journal of Geotechnical and Geoenvironmental Engineering*, vol. 134, no. 2, pp. 145–153, 2008.

[28] Z. Luo, S. Atamturktur, Y. Cai, and C. H. Juang, "Reliability analysis of basal-heave in a braced excavation in a 2-D random field," *Computers and Geotechnics*, vol. 39, pp. 27–37, 2012.

[29] Z. Luo, S. Atamturktur, Y. Cai, and C. H. Juang, "Simplified approach for reliability-based design against basal-heave failure in braced excavations considering spatial effect," *Journal of Geotechnical and Geoenvironmental Engineering*, vol. 138, no. 4, pp. 441–450, 2012.

[30] W.-S. Liu and S. H. Cheung, "Decoupled reliability-based geotechnical design of deep excavations of soil with spatial variability," *Applied Mathematical Modelling*, vol. 85, pp. 46–59, 2020.

[31] S. H. Wu, C. Y. Ou, J. Y. Ching et al., "Reliability-based design for basal heave in an excavation considering spatial variability," *GeoFlorida*, vol. 199, pp. 1914–1923, 2010.

[32] S.-H. Wu, C.-Y. Ou, J. Ching, and C. Hsein Juang, "Reliability-based design for basal heave stability of deep excavations in spatially varying soils," *Journal of Geotechnical and Geoenvironmental Engineering*, vol. 138, no. 5, pp. 594–603, 2012.

[33] F. Cai, K. Ugai, and T. Hagiwara, "Base stability of circular excavations in soft clay," *Journal of Geotechnical and Geoenvironmental Engineering*, vol. 128, no. 8, pp. 702–706, 2002.

[34] T.-N. Do, C.-Y. Ou, and A. Lim, "Evaluation of factors of safety against basal heave for deep excavations in soft clay using the finite-element method," *Journal of Geotechnical and Geoenvironmental Engineering*, vol. 139, no. 12, pp. 2125–2135, 2013.

[35] T.-N. Do and C.-Y. Ou, "Factors affecting the stability of deep excavations in clay with consideration of a full elastoplastic support system," *Acta Geotechnica*, vol. 15, no. 7, pp. 1707–1722, 2020.

[36] H. Faheem, F. Cai, and K. Ugai, "Three-dimensional base stability of rectangular excavations in soft soils using FEM," *Computers and Geotechnics*, vol. 31, no. 2, pp. 67–74, 2004.

[37] A. T. C. Goh, "Assessment of basal stability for braced excavation systems using the finite element method," *Computers and Geotechnics*, vol. 10, no. 4, pp. 325–338, 1990.

[38] A. T. C. Goh, "Estimating basal-heave stability for braced excavations in soft clay," *Journal of Geotechnical Engineering*, vol. 120, no. 8, pp. 1430–1436, 1994.

[39] A. T. C. Goh, "Basal heave stability of supported circular excavations in clay," *Tunnelling and Underground Space Technology*, vol. 61, pp. 145–149, 2017.

[40] F. Zhang and A. T. C. Goh, "Finite element analysis of basal heave stability for braced excavations in clays," *Japanese Geotechnical Society Special Publication*, vol. 2, no. 44, pp. 1551–1554, 2016.

[41] O. C. Zienkiewicz, C. Humpheson, and R. W. Lewis, "Associated and non-associated visco-plasticity and plasticity in soil mechanics," *Géotechnique*, vol. 25, no. 4, pp. 671–689, 1975.

[42] J. F. Wang, H. W. Xiang, and J. G. Yan, "Numerical simulation of steel sheet pile support structures in foundation pit excavation," *International Journal of Geomechanics*, vol. 19, Article ID 05019002, 2019.